

Brillouin-Mandelstam spectroscopy of standing spin waves in a ferrite waveguide

Michael Balinskiy, Fariborz Kargar, Howard Chiang, Alexander A. Balandin, and Alexander G. Khitun

Citation: [AIP Advances](#) **8**, 056017 (2018); doi: 10.1063/1.5007165

View online: <https://doi.org/10.1063/1.5007165>

View Table of Contents: <http://aip.scitation.org/toc/adv/8/5>

Published by the [American Institute of Physics](#)

Articles you may be interested in

[Effects of the magnetic field variation on the spin wave interference in a magnetic cross junction](#)

AIP Advances **8**, 056619 (2018); 10.1063/1.5007164

[Realization of spin wave switch for data processing](#)

AIP Advances **8**, 056628 (2018); 10.1063/1.5004992

[Experimental prototype of a spin-wave majority gate](#)

Applied Physics Letters **110**, 152401 (2017); 10.1063/1.4979840

[Spin-wave propagation in ultra-thin YIG based waveguides](#)

Applied Physics Letters **110**, 092408 (2017); 10.1063/1.4976708

[Spin waves with large decay length and few 100 nm wavelengths in thin yttrium iron garnet grown at the wafer scale](#)

Applied Physics Letters **111**, 012403 (2017); 10.1063/1.4991520

[Excitation of the three principal spin waves in yttrium iron garnet using a wavelength-specific multi-element antenna](#)

AIP Advances **8**, 056015 (2018); 10.1063/1.5007101



Brillouin-Mandelstam spectroscopy of standing spin waves in a ferrite waveguide

Michael Balinskiy,^a Fariborz Kargar, Howard Chiang, Alexander A. Balandin, and Alexander G. Khitun

Department of Electrical and Computer Engineering, University of California – Riverside, Riverside, California 92521, USA

(Presented 10 November 2017; received 30 September 2017; accepted 8 November 2017; published online 26 December 2017)

This article reports results of experimental investigation of the spin wave interference over large distances in the $\text{Y}_3\text{Fe}_2(\text{FeO}_4)_3$ waveguide using Brillouin-Mandelstam spectroscopy. Two coherent spin waves are excited by the micro-antennas fabricated at the edges of the waveguide. The amplitudes of the input spin waves are adjusted to provide approximately the same intensity in the central region of the waveguide. The relative phase between the excited spin waves is controlled by the phase shifter. The change of the local intensity distribution in the standing spin wave is monitored using Brillouin-Mandelstam light scattering spectroscopy. Experimental data demonstrate the oscillation of the scattered light intensity depending on the relative phase of the interfering spin waves. The oscillations of the intensity, tunable via the relative phase shift, are observed as far as 7.5 mm away from the spin-wave generating antennas at room temperature. The obtained results are important for developing techniques for remote control of spin currents, with potential applications in spin-based memory and logic devices. © 2017 Author(s). All article content, except where otherwise noted, is licensed under a Creative Commons Attribution (CC BY) license (<http://creativecommons.org/licenses/by/4.0/>). <https://doi.org/10.1063/1.5007165>

I. INTRODUCTION

Magnon spintronics is the emerging field of spintronics concerned with structures, devices, and circuits aimed to benefit from spin currents carried by spin waves.¹ The utilization of spin waves opens a new route to magnetic logic circuits.² There are several important advantages of using spin waves as information carriers. First, a combination of the magnetic memory with the spin wave bus makes possible a realization of the non-volatile logic circuits with zero static power consumption.³ Second, both the amplitude and the phase of the spin wave signal can be exploited for information transfer and processing. For instance, utilization of the phase for information encoding is efficient in certain types of the logic gates (e.g., MAJ, MOD2).¹ Finally, the spin wave interference offers a route to magnetic holographic devices^{4,5} enabling parallel magnetic bit read-out. Understanding of the spin wave interference phenomena is the key to development of novel magnonic devices.^{6–8} Brillouin-Mandelstam spectroscopy (BMS) is a powerful technique allowing for visualization of the spin waves in magnetic microstructures.^{9–11} In this work, we report results of the experimental study of the spin wave interference in the $\text{Y}_3\text{Fe}_2(\text{FeO}_4)_3$ waveguide using BMS. The rest of the paper is organized as follows. In Section II, we describe the test structure and experimental setup. In Section III, we present experimental data obtained by the electrical and optical measurements. The discussion and conclusions are given in Sections IV and V, respectively.

^aMichael Balinskiy, email: mbalinskyy@ece.ucr.edu

II. DEVICE STRUCTURE AND ELECTRICAL MEASUREMENTS

A schematic of the test structure and image of the experimental setup are shown in Fig. 1. The test structure consists of a YIG waveguide with two micro-antennas fabricated on top. The length of the channel is 16 mm, the width of the channel is 2 mm. The thickness of the YIG film is 9.6 μm . The saturation magnetization is $4\pi M_0 \approx 1750 \text{ Oe}$. The YIG film is epitaxially grown on top of a Gadolinium Gallium Garnett ($\text{Gd}_3\text{Ga}_5\text{O}_{12}$) substrate using the liquid phase epitaxy. The antennas are fabricated from a gold wire of thickness 60 μm and placed directly on top of the YIG surface near the edges of YIG waveguide. The antennas are orientated perpendicular to axis of waveguide. The antennas are fabricated from a gold wire of thickness 60 μm and placed directly on top of the YIG surface. Both antennas can be used for the spin wave excitation and detection. The spin wave excitation can be achieved by applying a radio frequency (RF) current through the antenna. The alternating electric current produces a non-uniform alternative magnetic field around the conducting contour, which, in turn, generates spin waves in the YIG channel under the spin wave resonance conditions. A detection of the spin waves is performed by measuring the inductive voltage in the receiving antenna. A propagating spin wave alters the magnetic flux from the surface and generates an inductive voltage in the antenna. The details of the inductive measurement technique can be found elsewhere.¹² The antennas are connected to a programmable network analyzer (PNA, Keysight N5221A). The device under test is placed inside an electromagnet GMW model 3472 - 70, pole cap 50 mm (2 inches) diameter tapered, which provides uniform bias magnetic field $\Delta H/H < 10^{-4}$ per 1 mm in the range from -2000 Oe to +2000 Oe. The in-plane magnetic field is directed perpendicular to the channel as depicted in Fig. 1(A).

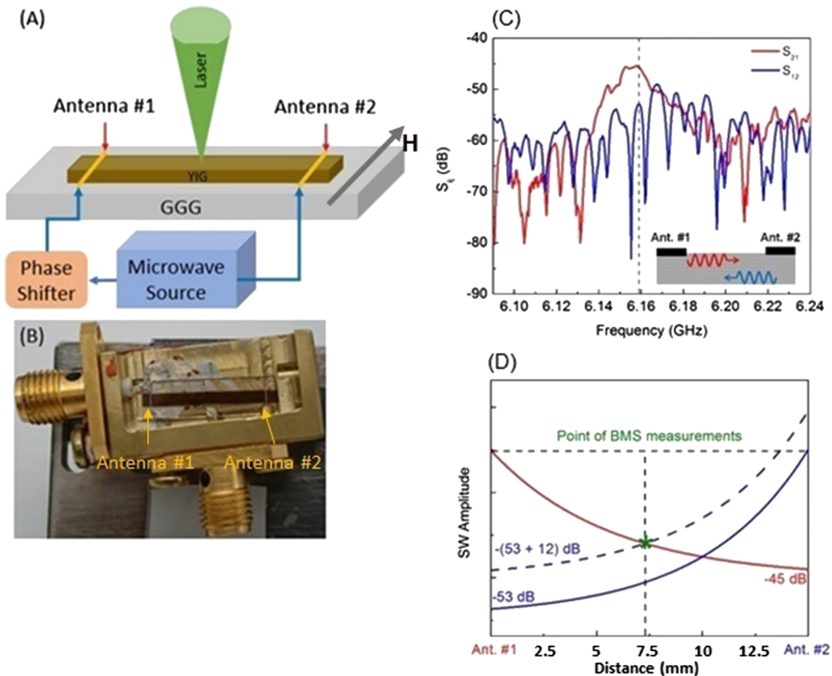


FIG. 1. (A) Schematic of the test structure and experimental setup. The test structure consists of a YIG waveguide with the following dimensions. The length of the channel is 16 mm, the width of the channel is 2 mm. The thickness of the YIG film is 9.6 μm . There are two micro-antennas fabricated on top of the waveguide. The antennas are connected to microwave source. (B) Photo of the device packaged for testing. (C) Experimental data for spin wave propagation between the antennas 1 and 2. The red curve shows the S_{21} parameter. The blue curve shows the S_{12} parameters. The green line corresponds to the chosen operational frequency $f = 6.159 \text{ GHz}$, where the both waves show maximum transmission (e.g., $S_{21} = -45 \text{ dB}$, $S_{12} = -53 \text{ dB}$). The inset illustrates the non-reciprocity in the spin wave propagation. (D) Illustration of the spin wave equalization process. The red and the blue solid curves depict the amplitudes of the propagating spin waves excited by the antennas 1 and 2, respectively. In order to equalize the BMS output in a given spot (i.e. the green star), we use an amplifier connected to antenna # 2. The dashed blue curve shows the amplitude of the spin wave excited at the antenna #2 after amplification.

The first set of experiments is aimed at confirming the spin wave generation by the antennas via the inductive voltage measurements, and finding the optimum operational frequency f and at the fixed bias magnetic field H . Based on our prior studies of the spin wave propagation in YIG films,^{7,13} we use the 1410 Oe bias magnetic field H and restrict the search region for the operation frequency from 6.0 GHz to 6.5 GHz. In Fig. 1(C), we present experimental data showing the spin wave propagation between the antennas (i.e., the S_{ij} parameter). The red curve and the blue curves in Fig. 1(C) correspond to the S_{21} and S_{12} parameters, respectively. In order to exclude the direct coupling between the antennas, the data are plotted after the subtraction to zero magnetic field ($S_{ij} = S_{ij}(H=1410 \text{ Oe}) - S_{ij}(H=0)$). The data show prominent spin wave propagation over the 15 mm distance at room temperature. At the same time, there is a significant non-reciprocity in the spin wave transport. For instance, the difference between S_{21} and S_{12} is about 10 dB at 6.16 GHz. This phenomenon is attributed to the specifics of magnetostatic surface spin wave propagation in thick films, where the spin waves propagating in the opposite directions are localized within the two opposite surfaces of the waveguide.¹⁴ The initial (pre-amplified) microwave power was about 3 dBm. No changes in the transmission characteristics were observed before and after the amplification comparable with the case of low power input -15 dBm. The latter indicates the linear regime of spin wave propagation. All further optical experiments are carried out at the fixed bias magnetic field $H = 1410 \text{ Oe}$, and operational frequency $f = 6.16 \text{ GHz}$.

III. BRILLOUIN-MANDELSTAM SPECTROSCOPY MEASUREMENTS

Two coherent spin waves propagating in the opposite direction form a standing wave. Our objective is to study the standing spin waves in a ferrite waveguide using BMS in order to determine the degree of control of the spin wave interference with the relative phase shift and estimating distances over which such control is efficient. BMS allows to detect magnon frequencies in the GHz range.¹⁵ The light source is a single frequency linearly polarized solid-state diode pumped laser operating at $\lambda = 532 \text{ nm}$. The experiments have been executed in backscattering configuration at normal incidence of laser light on the surface of the sample. The laser light has been focused on the sample by a lens with NA = 0.34. The scattered light has been collected with the same lens and directed to the high resolution six-pass tandem Fabry-Perot interferometer (JRS Instruments). The incident light is linearly p -polarized. Since the spin waves rotate the polarization of the incident photons by 90 degrees¹⁶ a polarizer in the scattered light path has been used to allow for passage of only the s -polarized light into the interferometer. Details of our BMS measurement procedures have been reported elsewhere.¹⁶⁻¹⁸

In order to observe the interference effects, the amplitudes of the interfering spin waves should be approximately the same at the point of observation. The amplitude of the spin wave signal decreases exponentially with the distance from the generating antenna. It would be a challenging and time-consuming task to find the place in the waveguide where the two spin waves produce the same BMS intensity. For this reason, we used an electric amplifier (Mini-Circuits, ZX60-83LN+) to equalize the spin wave amplitudes in a given spot. This technique is illustrated in Fig. 1(D). We selected a spot in the center of the waveguide, which is located at approximately the same distance from the spin wave generating antennas. Next, we detect the BMS signals produced by each antenna separately. The intensity of the BMS signals may vary significantly due to the difference in the spin wave propagation distance as well as due to the non-reciprocal spin wave propagation. To compensate the difference in BMS signal intensity, we use an amplifier before antenna #2. The amplitudes of the interfering spin waves were equalized by applying (+12 dB) amplification to antenna #2. The rest of the BMS measurements were accomplished at the given location on the waveguide and with the fixed gain.

We used both antennas for spin wave generation in order to study the interference of spin waves by BMS. The phase difference between the waves is controlled by the phase shifter (ARRA, model 9428A). In Fig. 2, we show the BMS spectra obtained for different positions of the phase shifter. The accumulation time for each spectrum is 10 minutes. At each experiment, we increase the phase difference by $\pi/5$ degrees. One can clearly see the Stokes and anti-Stokes signatures of magnons at the generator frequency. Fig. 3 presents the BMS intensity as a function of the phase difference

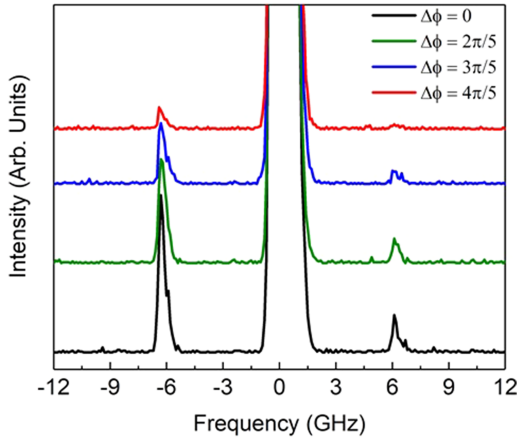


FIG. 2. Experimental data showing the BMS spectra for different phase difference between the interfering spin waves. There are four spectra corresponding to $\Delta\phi = 0\pi, 2\pi/5, 3\pi/5$, and $4\pi/5$.

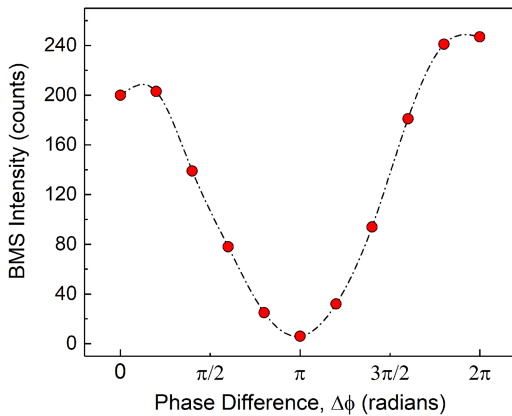


FIG. 3. Intensity of the BMS Stokes peak as a function of the phase difference between the two interfering spin waves. All the measurements are performed at room temperature.

between the interfering spin waves. The intensity oscillates, with the maxima corresponding to the constructive spin wave interference and the minimum corresponding to the destructive interference. One should note that the input power, applied to the spin wave generating antennas, remained the same during the experiment. The change in the BMS intensity reflects the change in the position of maxima and minima of the standing spin waves.

IV. DISCUSSION

The oscillation of the BMS intensity is observed about 7.5 mm away from the spin wave generating antennas at room temperature. The change in the phase difference between the interfering waves results in the magnetization redistribution within the standing spin wave. The obtained results suggest a promising approach for remote spin current control over large distances. The latter is beneficial for applications in the spin-based memory and logic devices. An example of the nonlinear magnetic cellular network, where magnetic elements are addressed by the interfering spin waves is described in Ref. 19. The use of BMS allows one to verify the changes in local magnetization caused by the remote control of the spin wave phase difference. The BMS mapping of the intensity distribution can help with the device structure optimization. One should note that BMS can only resolve standing spin waves with the period larger than the size of the optical spot. In our experiments, the diameter of the spot size is $\sim 25 \mu\text{m}$ while the spin wavelength exceeds 100 μm . One of the important questions is

related to the interference of two surface waves propagating on the opposite surfaces of the film as their decay profile depends on the sample thickness. It should also be noted that the spatial pattern across the width of the waveguide may be non-uniform.²⁰ This problem deserves a special investigation. The technique described in this work can be further used for investigation of the interaction between different types of spin waves in a variety of devices. The capability for an accurate control of the position of spin wave maxima and minima is important for logic devices that used the spin wave interference phenomena.

V. CONCLUSIONS

We reported results of BMS study of the spin wave interference in a YIG waveguide. The data show prominent BMS intensity oscillations as a function of the phase difference between the interfering spin waves. The intensity oscillations are observed approximately 7.5 mm away from the spin wave generating antennas at room temperature. The obtained results are important for developing techniques for remote control of spin currents, with potential applications in spin-based memory and logic devices.

ACKNOWLEDGMENTS

This was supported by the Spins and Heat in Nanoscale Electronic Systems (SHINES), an Energy Frontier Research Center funded by the U.S. Department of Energy, Office of Science, Basic Energy Sciences (BES) under Award # SC0012670.

- ¹ A. V. Chumak, V. I. Vasyuchka, A. A. Serga, and B. Hillebrands, "Magnon spintronics," *Nature Physics* **11**, 453–461 (2015).
- ² A. Khitun, M. Bao, and K. L. Wang, "Spin wave magnetic nanofabric: A new approach to spin-based logic circuitry," *IEEE Transactions on Magnetics* **44**, 2141–53 (2008).
- ³ A. Khitun and K. L. Wang, "Non-volatile magnonic logic circuits engineering," *Journal of Applied Physics* **110**, 034306–034310 (2011).
- ⁴ A. Khitun, "Spin wave phase logic," in *Cmos and Beyond: Logic Switches for Terascale Integrated Circuits* (2015), pp. 359–378.
- ⁵ F. Gertz, A. Kozhevnikov, Y. Filimonov, and A. Khitun, "Magnonic holographic memory," in *Magnetics, IEEE Transactions on* (2014), p. 4002905.
- ⁶ V. V. Kruglyak, S. O. Demokritov, and D. Grundler, "Magnonics," *Journal of Physics D-Applied Physics* **43**, 1–14 (2010).
- ⁷ M. Balynsky, A. Kozhevnikov, Y. Khivintsev, T. Bhowmick, D. Gutierrez, H. Chiang *et al.*, "Magnonic interferometric switch for multi-valued logic circuits," *Journal of Applied Physics* **121**, 024504 (2017).
- ⁸ M. Balynsky, D. Gutierrez, H. Chiang, A. Kozhevnikov, G. Dudko, Y. Filimonov *et al.*, "A magnetometer based on a spin wave interferometer," *Scientific Reports* **7**, 1–11 (2017).
- ⁹ B. Obry, P. Pirro, T. Bracher, A. V. Chumak, J. Osten, F. Ciubotaru *et al.*, "A micro-structured ion-implanted magnonic crystal," *Applied Physics Letters* **102**, 202403 (2013).
- ¹⁰ P. Pirro, T. Bracher, K. Vogt, B. Obry, H. Schultheiss, B. Leven *et al.*, "Interference of coherent spin waves in micron-sized ferromagnetic waveguides," *Physica Status Solidi B-Basic Solid State Physics* **248**, 2404–2408 (2011).
- ¹¹ V. E. Demidov, S. O. Demokritov, K. Rott, P. Krzysteczko, and G. Reiss, "Mode interference and periodic self-focusing of spin waves in permalloy microstrips," *Physical Review B* **77**, 064406 (2008).
- ¹² M. Covington, T. M. Crawford, and G. J. Parker, "Time-resolved measurement of propagating spin waves in ferromagnetic thin films," *Physical Review Letters* **89**, 237202-1-4 (2002).
- ¹³ A. Kozhevnikov, F. Gertz, G. Dudko, Y. Filimonov, and A. Khitun, "Pattern recognition with magnonic holographic memory device," *Applied Physics Letters* **106**, 142409 (2015).
- ¹⁴ R. W. Damon and J. R. Eshbach, "Magnetostatic modes of a ferromagnet slab," *Journal of Physics and Chemistry of Solids* **19**, 308–320 (1961).
- ¹⁵ M. M. Lacerda, F. Kargar, E. Aytan, R. Samnakay, B. Debnath, J. X. Li *et al.*, "Variable-temperature inelastic light scattering spectroscopy of nickel oxide: Disentangling phonons and magnons," *Applied Physics Letters* **110**, 202406 (2017).
- ¹⁶ T. Sebastian, K. Schultheiss, B. Obry, B. Hillebrands, and H. Schultheiss, "Micro-focused Brillouin light scattering: Imaging spin waves at the nanoscale," *Frontiers in Physics* **3**, 35 (2015).
- ¹⁷ F. Kargar, S. Ramirez, B. Debnath, H. Malekpour, R. K. Lake, and A. A. Balandin, "Acoustic phonon spectrum and thermal transport in nanoporous alumina arrays," *Applied Physics Letters* **107**, 171904 (2015).
- ¹⁸ F. Kargar, B. Debnath, J. P. Kakko, A. Saynatjoki, H. Lipsanen, D. L. Nika *et al.*, "Direct observation of confined acoustic phonon polarization branches in free-standing semiconductor nanowires," *Nature Communications* **7**, 13400 (2016).
- ¹⁹ A. Khitun, M. Q. Bao, and K. L. Wang, "Magnetic cellular nonlinear network with spin wave bus for image processing," *Superlattices and Microstructures* **47**, 464–483 (2010).
- ²⁰ C. Mathieu, V. T. Synogatch, and C. E. Patton, "Brillouin light scattering analysis of three-magnon splitting processes in yttrium iron garnet films," *Physical Review B* **67** (2003).